Ocean Systems Engineering, Vol. 2, No. 2 (2012) 115-135
DOI: http://dx.doi.org/10.12989/ose.2012.2.2.115

Response of square tension leg platforms to hydrodynamic forces

A.M. Abou-Rayan[1], Ayman A. Seleemah*[2] and Amr R. El-gamal[1]

[1]*Civil Engineering Tec. Dept., Faculty of Engineering, Benha Univ., Egypt*
[2]*Structural Engineering Dept., Faculty of Engineering, Tanta Univ., Egypt*

(Received September 5, 2011, Revised June 1, 2012, Accepted June 7, 2012)

Abstract. The very low natural frequencies of tension leg platforms (TLP's) have raised the concern about the significance of the action of hydrodynamic wave forces on the response of such platforms. In this paper, a numerical study using modified Morison equation was carried out in the time domain to investigate the influence of nonlinearities due to hydrodynamic forces and the coupling effect between surge, sway, heave, roll, pitch and yaw degrees of freedom on the dynamic behavior of TLP's. The stiffness of the TLP was derived from a combination of hydrostatic restoring forces and restoring forces due to cables and the nonlinear equations of motion were solved utilizing Newmark's beta integration scheme. The effect of wave characteristics such as wave period and wave height on the response of TLP's was evaluated. Only uni-directional waves in the surge direction was considered in the analysis. It was found that coupling between various degrees of freedom has insignificant effect on the displacement responses. Moreover, for short wave periods (i.e., less than 10 sec.), the surge response consisted of small amplitude oscillations about a displaced position that is significantly dependent on the wave height; whereas for longer wave periods, the surge response showed high amplitude oscillations about its original position. Also, for short wave periods, a higher mode contribution to the pitch response accompanied by period doubling appeared to take place. For long wave periods, (12.5 and 15 sec.), this higher mode contribution vanished after very few cycles.

Keywords: compliant structures; tension leg platforms; hydrodynamic wave forces; coupling effect; wave period; wave height

1. Introduction

Since the late 1940's, when offshore drilling platforms were first used in the gulf of Mexico there has been a large increase in the number of offshore platforms put into service. Production activities at their sites are generally carried out using fixed offshore platforms, which are valid only for shallow waters. For deep waters, however, it is uneconomic to build a stiff jacket or gravity type platform to resist the wave loads. Therefore, the compliant platforms, an engineering idea to minimize the structure resistance to environmental loads by making the structure flexible, have been introduced. A tension leg platform (TLP) is one of the compliant structures which are well established in offshore industry. The TLP is basically a floating structure moored by vertical cables or "tethers". Tethers are pre-tensioned to the sea floor due to the excess buoyancy of the platform.

*Corresponding author, Professor, E-mail: seleemah55@yahoo.com

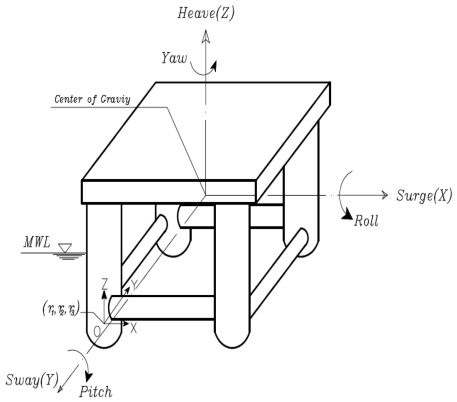

Fig. 1 The global and local coordinate system of TLP

This tension fluctuates due to variable submergence, wind gustiness, wave loading and resulting coupled response. The instantaneous tension in tethers acts as a restoring force.

The TLP can be modeled as a rigid body with six degrees of freedom (refer to Fig. 1), which can be conveniently divided into two categories, those controlled by the stiffness of tethers, and those controlled by the buoyancy. The former category includes motion in the vertical plane and consists of heave, roll and pitch; whereas the latter comprises the horizontal motions of surge, sway and yaw .The natural periods of motion in the horizontal plane are high, whereas in the vertical plane the periods are low. Generally, the surge and sway motions are predominantly high for head seas due to the combined actions of wind, waves and currents. However, due to coupling among various degrees of freedom and relatively low damping of hydrodynamic origin in the vertical plane motion, a complete analysis of a six degree-of-freedom system subjected to wind, waves and currents is desirable. Moreover, the structural flexibility in the horizontal motions causes nonlinearity in the structural stiffness matrix because of large deformations.

The natural periods of the horizontal plane motions are higher than typical wave period which precludes resonance with the wave diffraction forces. However, the wave-induced low frequency forces, namely the wave drift forces, could be close (to some extent) to the natural periods of motion in the horizontal plane causing a significant response of a TLP despite the low amplitude of these forces. The maximum TLP response at low frequencies in various extreme environmental conditions is of primary importance from the point of view of platform stability, serviceability and fatigue of tethers.

A number of studies have been conducted on the dynamic behavior of TLP's under both regular and random waves, (Taudin 1978, Denis and Heaf 1979, Tan and De Boom 1983). The majority of these studies deal with the two dimensional behavior of the platform. Few investigations, however considered all the six degrees of freedom of the platform in describing its dynamic behavior, Morgan and Malaeb (1983) Chandrasekaran and Roy (2005). They presented phase space studies of offshore structures subjected to nonlinear dynamic loading through Poincare maps for certain hydrodynamic parameters. Bhattachatya *et al*. (2004) investigated coupled dynamic behavior of a mini TLP giving special attention to hull-tether coupling. Ketabdari and Ardakani (2005) developed a computer program to evaluate the dynamic response of sea-star TLP to regular wave forces considering coupling between different degrees of freedom. Wave forces were computed numerically using linear wave theory and Morison equation, neglecting diffraction effects due to

small ratio of diameter to wave length. Lee and Wang (2000) investigated the dynamic behavior of a TLP with a net-cage system with a simplified two-dimensional modeling. They found that there is a close relationship between the dynamic behavior of the platform and the net-cage features. Low (2009) presented a formulation for the linearization of the tendon restoring forces of a TLP. Chandrasekaran *et al*. (2007a) conducted dynamic analysis of triangular TLP models at different water depths under the combined action of regular waves and an impulse load affecting the TLP column. Chandrasekaran *et al*. (2007b) focused on the response analysis of triangular tension leg platform (TLP) for different wave approach angles and studied its influence on the coupled dynamic response of triangular TLPs. Kurian *et al*. (2008a) developed a numerical study on the dynamic response of square TLPs subjected to regular and random waves. They also conducted parametric studies with varying parameters such as water depth, pretension, wave angle and position of center of gravity. Kurian *et al*. (2008b) developed a numerical study on determining the dynamic responses of square and triangular TLPs subjected to random waves. They found that the responses of triangular TLPs are much higher than those of square TLP. Recently, Yang and Kim (2010) developed a numerical study of the transient effect of tendon disconnection on the global performance of an extended tension leg platform (ETLP) during harsh environmental conditions of the gulf of Mexico.

In this paper, a numerical study was conducted to investigate the dynamic response of a rectangular TLP (shown in Fig. 2) under hydrodynamic forces considering all degrees of freedom of the system. The analysis was carried out using modified Morison equation in the time domain with

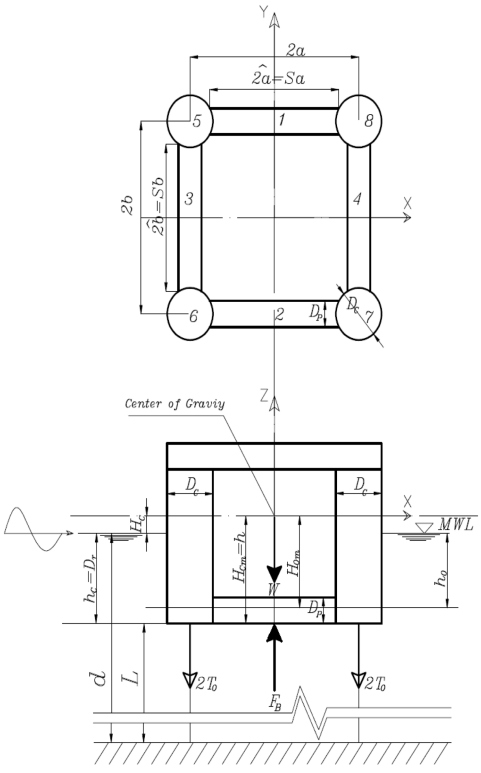

Fig. 2 The Square TLP (plan and elevation)

water particle kinematics using Airy's linear wave theory. The influence of nonlinearities due to hydrodynamic forces and the coupling effect between surge, sway, heave, roll, pitch and yaw degrees of freedom on the dynamic behavior of TLP's was investigated. The stiffness of the TLP was derived from a combination of hydrostatic restoring forces and restoring forces due to cables and the nonlinear equations of motion were solved utilizing Newmark's beta integration scheme. The effect of wave characteristics such as wave period and wave height on the response of TLP's was evaluated. Only uni-directional waves in the surge direction was considered in the analysis.

2. Structural idealization and assumptions

The general equation of motion of the rectangular configuration TLP model under a regular wave is given as

$$[M]\{\ddot{x}\} + [C]\{\dot{x}\} + [K]\{x\} = \{F(t)\} \tag{1}$$

Where, $\{x\}$ is the structural displacement vector, $\{\dot{x}\}$ is the structural velocity vector, $\{\ddot{x}\}$ is the structural acceleration vector; $[M]$ is the structure mass matrix; $[C]$ is the structure damping matrix; $[K]$ is the structure stiffness matrix; and $\{F(t)\}$ is the hydrodynamic force vector.

The mathematical model derived in this study assumes that the platform and the tethers are treated as a single system and the analysis is carried out for the six degrees of freedom under different environmental loads where wave forces are estimated at the instantaneous equilibrium position of the platform utilizing Morison's equation and using Airy's linear wave theory. Wave force coefficients, C_d and C_m, are the same for the pontoons and the columns and are independent of frequencies as well as constant over the water depth. The following assumptions were made in the analysis.

1. Change in pre-tension is calculated at each time step, so the equation of equilibrium at each time step modifies the elements of the stiffness matrix.
2. The platform has been considered symmetrical along the surge axis. Directionality of wave approach to the structure has been ignored in the analysis and only a uni-directional wave train has been considered.
3. The damping matrix has been assumed to be mass and stiffness proportional.
4. The force on tethers (gravity, inertia, drag, hydrostatic and hydrodynamic forces) has been neglected because of its small area and also the tether curvature is not significant in motion; only the axial forces acting on tethers have been considered.
5. Hydrodynamic forces on connecting members and mooring legs have been neglected.
6. The wave, current and structure motions are taken to occur in the same plane and in the same direction, the interaction of wave and current has been ignored.
7. Integration of hydrodynamic inertia and drag forces are carried out up to the actual level of submergence, when variable submergence is considered.

It should be mentioned that, the analysis is limited to unidirectional wave force acting on symmetrical configuration. Also, current was assumed to be taken as 10% of wind velocity at a height of 10 m above the water surface. These two assumptions are not valid for high seas conditions.

3. Development of rectangular TLP model

3.1 Draft evaluation

At the original equilibrium position, Fig. 2, summation of forces in the vertical direction gives:

$$W + T = F_B \tag{2}$$

So

$$W + (4T_o) = F_B \tag{3}$$

$$F_B = \rho\pi g(4D_c^2 D_r + 2D_p^2 s_a + 2D_p^2 s_b) \tag{4}$$

From Eq. (4), we find that

$$D_r = \frac{[\{(W+T)/(0.25\rho\pi g)\} - 2D_p^2 s_a - 2D_p^2 s_b]}{4D_c^{\,2}} \tag{5}$$

where, F_B is the total buoyancy force; W is the total weight of the platform in air; T is the total instantaneous tension in the tethers; T_o is the initial pre-tension in the tether; r is the mass density of sea water; D_c is the diameter of TLP columns; D_p is the diameter of pontoon; S_a and S_b are the length of the pontoon between the inner edges of the columns in the x and y directions, respectively; and D_r is the draft.

3.2 Stiffness matrix of rectangular TLP configuration

The stiffness of the platform is derived from a combination of hydrostatic restoring forces and restoring forces due to the cables. Restoring force for motions in the horizontal plane (surge, sway, and yaw) are the horizontal component of the pretension in the cables, while restoring forces for motions in the vertical plane arise primarily from the elastic properties of the cables, with a relatively small contribution due to hydrostatic forces. The coefficients, *Kij*, of the stiffness matrix of rectangle TLP are derived from the first principles as the reaction in the degree of freedom *i,* due to unit displacement in the degree of freedom *j*, keeping all other degrees of freedom restrained. The coefficients of the stiffness matrix have nonlinear terms. Moreover, the tether tension changes due to the motion of the TLP in different degrees of freedom leads to a response-dependent stiffness matrix. The coefficients of the stiffness matrix [K] of a rectangle TLP are

$$[K] = \begin{bmatrix} K_{11} & 0 & 0 & 0 & K_{15} & 0 \\ 0 & K_{22} & 0 & K_{24} & 0 & 0 \\ K_{31} & K_{32} & K_{33} & K_{34} & K_{35} & K_{36} \\ 0 & K_{42} & 0 & K_{44} & 0 & 0 \\ K_{51} & 0 & 0 & 0 & K_{55} & 0 \\ 0 & 0 & 0 & 0 & 0 & K_{66} \end{bmatrix} \tag{6}$$

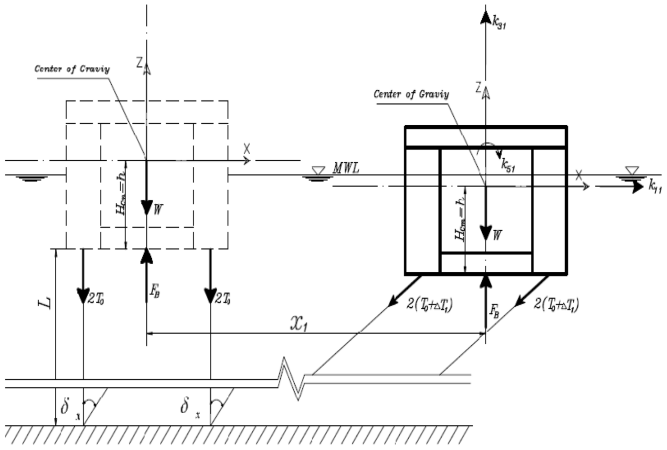

Fig. 3 The Surge displacement in a rectangular TLP

and can be determined as following

Surge (1) direction

The coefficients of the first column of the restoring force matrix are found by giving a unity x displacement in the x-direction (surge) as shown in Fig. 3. The increase in the initial pre-tension in each leg is given by

$$\Delta T_1 = \frac{E \times A \times \Delta L}{L} \tag{7}$$

$$\Delta L = \sqrt{x_1^2 + L^2} - L \tag{8}$$

where A is the cross-sectional area of the tether; E is the Young's Modulus of the tether; ΔT_1 is the increase in the initial pre-tension due to the arbitrary displacement given in the surge degree of freedom; L is the length of the tether; and x_1 is the arbitrary displacement in the surge degree of freedom. Equilibrium of forces in different directions gives

$$K_{11} = \frac{4(T_o + \Delta T_1)}{\sqrt{x_1^2 + L^2}} \tag{9}$$

$$K_{31} = \frac{\left[4T_o\left(\frac{L}{\sqrt{x_1^2 + L^2}} - 1\right) + 4\Delta T_1 \frac{L}{\sqrt{x_1^2 + L^2}}\right]}{x_1} \tag{10}$$

$$\sum M_X = O = K_{41}\, x_1 \Rightarrow K_{41} = O \tag{11}$$

$$K_{51} = (-K_{11}\, h) \tag{12}$$

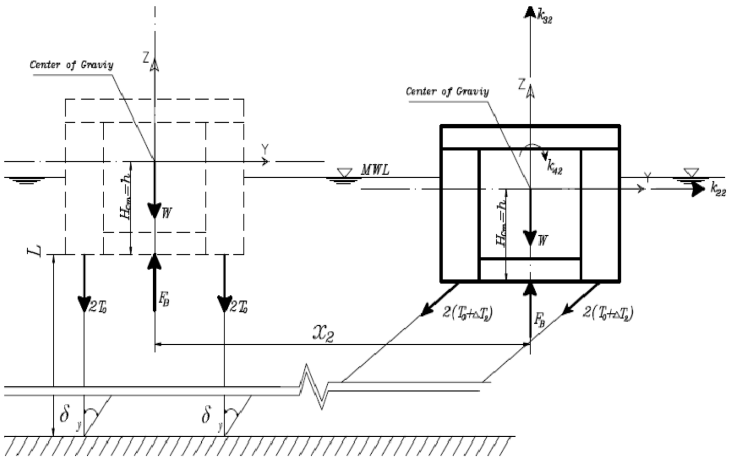

Fig. 4 The Sway displacement in a rectangular TLP

The negative sign occurs due to the counterclockwise moment, where, h is the distance between the center of mass and the bottom of the platform (see Fig. 3).

$$\sum M_z = O = K_{61}x_1 \Rightarrow K_{61} = O \tag{13}$$

Sway (2) direction

The coefficients of the second column of the restoring force matrix are found in a similar manner by giving a unity y displacement in the y-direction (sway) as shown in Fig. 4.

$$K_{12} = 0,\ K_{52} = 0 \text{ and } K_{62} = 0 \tag{14}$$

$$K_{22} = \frac{4(T_o + \Delta T_2)}{\sqrt{x_2^2 + L^2}} \tag{15}$$

$$K_{32} = \frac{\left[4T_o\left(\frac{L}{\sqrt{x_2^2+L^2}} - 1\right) + 4\Delta T_2 \frac{L}{\sqrt{x_2^2+L^2}}\right]}{x_2} \tag{16}$$

$$K_{42} = -hK_{22} \tag{17}$$

Where ΔT_2 is the increase in tension due to sway and is given by

$$\Delta T_2 = \frac{E \times A \times \Delta L}{L} \tag{18}$$

$$\Delta L = \sqrt{x_2^2 + L^2} - L \tag{19}$$

Note that δ_x and δ_y shown in Figs. 3 and 4 are the angles of inclination of the cables with respect to the vertical when under surge and sway movements, respectively.

Heave (3) direction

The third column is derived by giving the structure an arbitrary displacement in the z direction (heave). The sum of the forces in the all directions yield

$$K_{13} = K_{23} = K_{43} = K_{53} = K_{63} = 0 \tag{20}$$

$$K_{33} = 4\frac{EA}{L} + 4\frac{\pi D_c^2}{4}\rho g \tag{21}$$

Roll (4) direction

The coefficients in the fourth column of the restoring force matrix are found by giving the structure in arbitrary rotation x_4 about the x-axis as shown in Fig. 5. Summation of the moments of the resulting forces about the x-axis yields

$$K_{14} = K_{54} = K_{64} = 0 \tag{22}$$

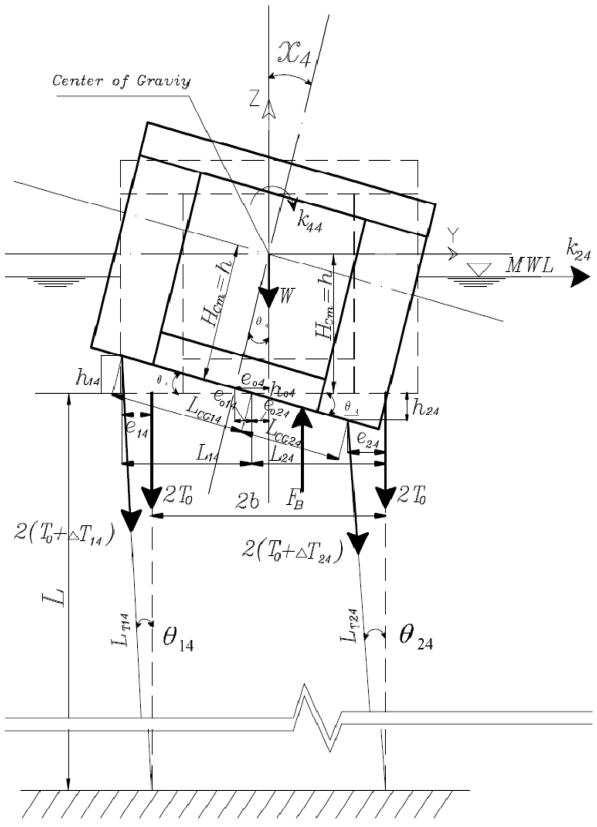

Fig. 5 The Roll displacement in a rectangular TLP

Taking summation of forces in y-axis we find that

$$K_{24} = \frac{[(2(T_o + \Delta T_{14})Sin\,\theta_{14} + 2(T_o + \Delta T_{24})Sin\,\theta_{14})]}{x_4} \tag{23}$$

By taking summation of forces about *z*-axis we find that

$$\Rightarrow k_{34} = [(2(T_o + \Delta T_{14})\mathrm{Cos}\,\theta_{14} + 2(T_o + \Delta T_{24})Cos\,\theta_{24} - 4T_o)]/x_4 \tag{24}$$

and taking summation of moments about *x* axis we get

$$K_{44} = \begin{bmatrix} (2(T_o + \Delta T_{14})Cos\,\theta_{14}\,(b + e_{14}) - 2(T_o + \Delta T_{24})Cos\,\theta_{24}\,(b - e_{24}) + F_B \times e_{o4}) \\ + (2(T_o + \Delta T_{24})Sin\,\theta_{24}\,(H - h_{24}) + 2(T_o + \Delta T_{14})Sin\,\theta_{14} \times (H - h_{14})) \end{bmatrix} / x_4 \tag{25}$$

Pitch (5) direction

The coefficients in the fifth column of the restoring force matrix are found by giving the structure an arbitrary rotation x_5 about the y-axis (see Fig. 6). Summation of the moments of the resulting forces about the *y*-axis gives

$$K_{25} = K_{45} = K_{65} = 0 \tag{26}$$

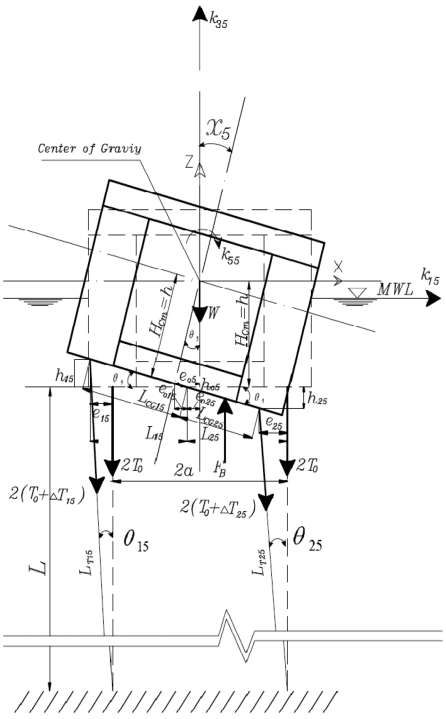

Fig. 6 The Pitch displacement in a rectangular TLP

Taking summation of forces in the x-direction, we find that

$$K_{15} = \frac{[2(T_o + \Delta T_{15})Sin\theta_{15} + 2(T_o + \Delta T_{25})Sin\theta_{25}]}{x_5} \tag{27}$$

Taking summation of forces in the z-direction, we obtain

$$\Rightarrow k_{35} = [(2(T + \Delta T_{15})Cos\theta_{15} + 2(T_o + \Delta T_{25})Cos\theta_{25} - 4T)]/x_5 \tag{28}$$

By taking summation of moments about y-axis then

$$K_{55} = \left[\begin{array}{c} 2(T_o + \Delta T_{15})Cos\theta_{15}\,(a + e_{15}) - 2(T_o + \Delta T_{25})Cos\theta_{25}\,(a - e_{25}) \\ + F_B \times e_{o5} + (2(T_o + \Delta T_{25})Sin\theta_{25}(H - h_{25}) + 2(T_o + \Delta T_{15})Sin\theta_{15} \times (H - h_{15})) \end{array} \right] / x_5 \tag{29}$$

Yaw (6) direction

By giving an arbitrary rotation x_6 in the yaw degree of freedom, the sixth column of the restoring force matrix can be obtained (see Fig. 7). We can find that

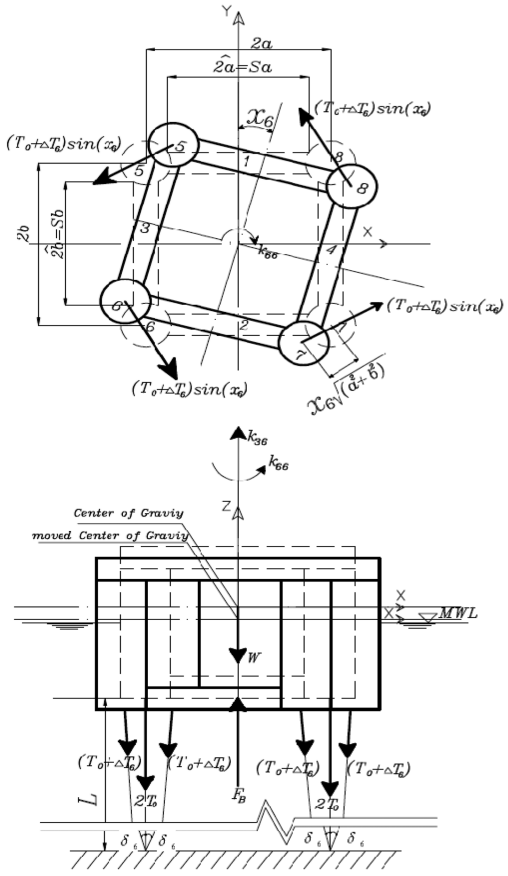

Fig. 7 The Yaw displacement in a rectangular TLP

$$K_{16} = K_{26} = K_{46} = K_{56} = 0 \tag{30}$$

By taking summation of moment about z-axis we find that

$$K_{66} = 4(T_o + \Delta T_6)\frac{(a^2+b^2)}{L^2 + x_6^2(a^2+b^2)} \tag{31}$$

Finally, through summation of forces in the vertical direction one obtains

$$K_{36} = \left[4T_o\left(\frac{L}{L^2 + x_6^2(a^2+b^2)} - 1\right) + 4\Delta T_6\left(\frac{L}{L^2 + x_6^2(a^2+b^2)}\right)\right] / x_6 \tag{32}$$

Where $\Delta T_6 = \frac{AE}{L}(L^2 + x_6^2(a^2+b^2) - L)$ is the change in tether tension force due to yaw displacement.

The overall stiffness matrix given by Eq. (6) shows

1. The presence of off-diagonal terms, which reflects the coupling effect between the various degrees of freedom.
2. The coefficients depend on the change in the tension of the tethers, which is affecting the buoyancy of the system. Hence, the matrix is response dependent.

Hence, during the dynamic analysis, the [*K*] matrix is not constant for all time instants, but its components are continuously changing at each time step depending upon the response values at the previous time step.

3.3 Mass matrix, [M]

The mass matrix is assumed to be lumped at each degree of freedom. Hence, it is diagonal in nature and is constant. However, the added mass, *M*a, due to the water surrounding the structural members has been considered up to the mean sea level (MSL) and arising from the modified Morison equation. The presence of off diagonal terms in the mass matrix indicates a contribution of the added mass due to the hydrodynamic loading. The fluctuating components of added mass due to the variable submergence of the structure in water is considered in the force vector depending upon whether the sea surface elevation is above or below the MSL.

The added mass matrix of submerged portion of an arbitrarily inclined cylinder can be expressed in terms of the direction cosines, Patel (1989). If the cylinder is located between coordinates (*X1*, *Y1*, *Z1*) and (*X2*, *Y2*, *Z2*) relative to principal platform axis, then direction cosines can be defined as follows

$$cos\alpha = \frac{X_2 - X_1}{L},\ cos\beta = \frac{Y_2 - Y_1}{L},\ cos\gamma = \frac{Z_2 - Z_1}{L} \tag{33}$$

The one-half of the symmetrical added mass matrix coefficients are

$$M_{a11} = \int_L (\rho C_a A sin^2\alpha) dL \tag{34}$$

$$M_{a22} = \int_L (\rho C_a A \sin^2 \beta) dL \tag{35}$$

$$M_{a13} = M_{a31} = \int_L -(\rho C_a A \cos\alpha \cos\gamma) dL \tag{36}$$

$$M_{a32} = M_{a23} = \int_L -(\rho C_a A \cos\beta \cos\gamma) dL \tag{37}$$

$$M_{a15} = M_{a51} = M_{a11}\overline{Z} - M_{a13}\overline{X} \tag{38}$$

$$M_{a24} = M_{a22}\overline{Z} = M_{a13}\overline{Y} \tag{39}$$

$$M_{a33} = \int_L (\rho C_a A \sin^2 \gamma) dL \tag{40}$$

$$M_{a35} = M_{a53} = M_{a13}\overline{Z} - M_{a33}\overline{X} \tag{41}$$

$$M_{a34} = M_{a43} = M_{a23}\overline{Z} - M_{a33}\overline{Y} \tag{42}$$

$$M_{a55} = M_{a11}\overline{X_m^2} - 2M_{a13}(ZX)_m + M_{a33}\overline{Z_m^2} \tag{43}$$

$$M_{a44} = M_{a22}\overline{Y_m^2} - 2M_{a23}(ZX)_m + M_{a33}\overline{Z_m^2} \tag{44}$$

$$M_{a66} = M_{a22}\overline{Y_m^2} + M_{a11}\overline{X_m^2} \tag{45}$$

$$M_{a16} = M_{a61} = -M_{a11}\overline{Y} \tag{46}$$

$$M_{a26} = M_{a62} = -M_{a22}\overline{X} \tag{47}$$

Where

$$A = \frac{\pi D^2}{4} \tag{48}$$

$$\overline{X} = \frac{X_1 + X_2}{2} \tag{49}$$

$$\overline{Y} = \frac{Y_1 + Y_2}{2} \tag{50}$$

$$\overline{Z} = \frac{Z_1 + Z_2}{2} \tag{51}$$

$$\overline{X_m^2} = \frac{X_1^2 + X_1X_2 + X_2^2}{3} \tag{52}$$

$$\overline{Y_m^2} = \frac{Y_1^2 + Y_1 Y_2 + Y_2^2}{3} \tag{53}$$

$$\overline{Z_m^2} = \frac{Z_1^2 + Z_1 Z_2 + Z_2^2}{3} \tag{54}$$

$$(ZX)_m = \frac{2Z_1X_1 + 2Z_2X_2 + Z_1X_2 + Z_2X_1}{6} \tag{55}$$

$$(ZY)_m = \frac{2Z_1X_1 + 2Z_2X_2 + Z_1X_2 + Z_2X_1}{6} \tag{56}$$

The loading will be attracted only in the surge, heave and pitch degrees of freedom due to the unidirectional wave acting in the surge direction on a symmetric configuration of the platform about the x and z axes. Therefore, the mass matrix can be written as

$$[M] = \begin{bmatrix} M+M_{a11} & 0 & M_{a13} & 0 & M_{a15} & M_{a16} \\ 0 & M+M_{a22} & M_{a23} & M_{a24} & 0 & M_{a26} \\ M_{a31} & M_{a32} & M+M_{a33} & M_{a34} & M_{a35} & 0 \\ 0 & M_{a42} & M_{a43} & Mr_x^2+M_{a44} & 0 & 0 \\ M_{a51} & 0 & M_{a53} & 0 & Mr_y^2+M_{a55} & 0 \\ M_{a61} & M_{a62} & 0 & 0 & 0 & Mr_z^2+M_{a66} \end{bmatrix} \tag{57}$$

Where, M is the mass of the body, r_x, r_y, and r_z are the radii of gyrations about the *x, y, and z*-axes, respectively.

3.4 Structural damping [C]

Damping was presented in the form of alpha and beta damping (Rayleigh Damping). The damping matrix $[C]$ is calculated by using alpha and beta constants as multipliers to the mass matrix $[M]$ and stiffness matrix $[K]$, respectively.

$$[C] = \alpha [M] + \beta [K] \tag{58}$$

The values of α and β are calculated based on typical modal damping ratios, ξ_i.

3.5 Hydrodynamic force vector, {F (t)} on rectangular TLP

The problem of suitable representation of the wave environment or more precisely the wave loading is a problem of prime concern. Once the wave environment is evaluated, wave loading on

the structure may be computed based on suitable theory. In this study the water particle position η is determined according to Airy's linear wave theory as following

$$\eta(x,t) = A_m cos(kx - \omega t - \varphi) \tag{59}$$

Where A_m is the amplitude of the wave; k is the wave number; ω is the wave frequency; x is the horizontal distance from the origin; and φ is the wave phase angle. This description assumes a wave form which have small height, H, in comparison to its wave length, λ, and water depth, d. In order to incorporate the effect of variable submergence which is an important aspect of hydrodynamic loading on TLP, instantaneous sea surface elevation is taken as the still water level (or water depth). The fluctuating free surface effect can be significant when the wave height cannot be ignored compared to the water depth.

The hydrodynamic force vector is calculated in each degree of freedom according to modified Morison's equation which takes into account the relative velocity and acceleration between the structure and the fluid particles. It is also worth mentioning that the ratio d/H can be related to d/λ. Based on the limiting heights of breaking waves, it become unstable and break when $H/\lambda \geq$ o.1, (λ is the wave length).

$$dF = \left[\rho C_m A_s\left(\frac{du}{dt} - \frac{dx^{\cdot}}{dt}\right)\right] + \left[\rho C_d D\left|U - \frac{dx}{dt}\right|\left(U - \frac{dx}{dt}\right)\right] - \left[(C_m - 1)\rho A_s \frac{dx^{\cdot}}{dt}\right] \tag{60}$$

and

$$U = u + \left(\frac{d+z}{d} Uc\right) \tag{61}$$

Where A_s is the cross-sectional area; C_m is the inertia coefficient; U is the undisturbed fluid velocity; Uc is the current velocity, if exist; and C_d is the drag coefficient. Note that in Eq. (60), the first term represents the inertia force, the second term represents the drag force, and the last term represents the added mass force. The term $|U|$ is written in this form to ensure that the drag force component is in the same direction as the velocity.

The components of the normal velocity and acceleration vectors for a segment of an arbitrarily inclined cylinder can be expressed as

$$u_x = (u - x_1^{\cdot}) sin^2\alpha - (w - x_2^{\cdot}) \cos\alpha \cos\gamma \tag{62}$$

$$u_z = (w - x_3^{\cdot}) sin^2\gamma - (u - x_1^{\cdot}) \cos\alpha \cos\gamma \tag{63}$$

$$u_x^{\cdot} = u^{\cdot} sin^2\alpha - w^{\cdot} \cos\alpha \cos\gamma \tag{64}$$

$$u_z^{\cdot} = w^{\cdot} sin^2\gamma - u^{\cdot} \cos\alpha \cos\gamma \tag{65}$$

Where u,w and $u^{\cdot}$, $w^{\cdot}$ are the horizontal and vertical water particle velocities and accelerations, respectively.

Wave and current loading naturally occur simultaneously and current direction may not coincide with wave direction and may vary with depth. The speed may also change with depth. To present a

realistic description, a profile which may vary in both magnitude and direction with depth is considered. The current velocity is taken about 10% of wind velocity at a height of 10 m above the water surface.

For the uni-directional wave train in the surge direction, the force vector $\{F(t)\}$, is given by

$$F(t) = \{F_{11} \;\; F_{21} \;\; F_{31} \;\; F_{41} \;\; F_{51} \;\; F_{61}\}^T \tag{66}$$

Since the wave is unidirectional, there would be no force in the sway degree-of-freedom F_{21} and hence there will be no moment in the roll degree of-freedom F_{41}. Because of the vertical water particle velocity and acceleration, the heave degree-of-freedom would experience wave force F_{31}. The force in the surge direction F_{11} on the vertical members will cause moment in the pitch degree-of-freedom F_{51}. However, forces in the surge degree-of-freedom are symmetrical about the X axis (due to the symmetry of the platform to the approaching wave) and there will be no net moment caused in the yaw degree-of-freedom F_{61}.

3.6. Solution of the equation of motion in the time domain

The equation of motion is coupled and nonlinear and can be written as

$$[M]\{\ddot{x}(t+\Delta t)\} + [C]\{\dot{x}(t+\Delta t)\} + [K]\{x(t+\Delta t)\} = \{F(t+\Delta t)\} \tag{67}$$

Eq. (67) is nonlinearly coupled, because of the presence of structural displacement, velocity and acceleration in the right hand side of the equation. Therefore, the force vector should be updated at each time step to account for the change in the tether tension. To achieve this response variation a time domain analysis is carried out. The Newmark's beta time integration procedure is used in a step wise manner. This procedure was developed by Newmark together with a family of time-stepping methods based on the following equations.

$$\dot{x}(t+\Delta t) = \dot{x}(t) + [(1-\gamma)\Delta t]\ddot{x}(t) + \gamma(\Delta t)\ddot{x}(t+\Delta t) \tag{68}$$

$$x(t+\Delta t) = [x(t) + (\Delta t)\dot{x}(t) + [(0.5-\beta)(\Delta t)^2]\ddot{x}(x) + [\beta(\Delta t)^2]\ddot{x}(t+\Delta t)] \tag{69}$$

The parameters β and γ define the variation of acceleration $\ddot{x}$ over time step Δt and determine the stability and accuracy characteristics of the method. Typical selection for γ is 1/2 and $1/6 \le \beta \le 1/4$ is satisfactory from all points of view, including accuracy.

The two special cases of Newmark's method that are commonly used are

(1) Average acceleration method in which the value of γ is 1/2, $\beta = 1/4$ where, this method is unconditionally stable.

(2) Linear acceleration method in which the value of γ is 1/2, $\beta = 1/4$ where, this method is conditionally stable.

The first method was utilized in this study. The procedure of this method is summarized as solving Eq. (69) for $\ddot{x}(t+\Delta t)$ in terms of $x(t+\Delta t)$ and then substituting for $\ddot{x}(t+\Delta t)$ into Eqn 68 we obtain equations for $\ddot{x}(t+\Delta t)$ and $\dot{x}(t+\Delta t)$, each in terms of unknown $x(t+\Delta t)$ only. These two relations for $\dot{x}(t+\Delta t)$ and $\ddot{x}(t+\Delta t)$ are substituted into Eq. (67) to solve for $x(t+\Delta t)$ after which, using Eqs. (68) and (69), $\ddot{x}(t+\Delta t)$ and $\dot{x}(t+\Delta t)$ can also be calculated at each step.

The following values are updated
(a) stiffness coefficients which varies with tether tension;
(b) added mass which varies with sea surface fluctuations;
(c) wave forces at the instantaneous position of the displaced structure.

4. Results and discussion

A numerical scheme was developed using MATLAB software where solution based on Newmark's beta method was obtained. A major concern was about the effect of the coupling of the degrees of freedom and about its rule in influencing some of the response behaviors critically. Thus, numerical studies for evaluating the coupled and uncoupled responses of the square TLP under regular waves have been carried out. Coupling of various degrees-of-freedom was taken into consideration by considering the off-diagonal terms in stiffness matrix [K]. On the other hand, these off-diagonal terms were neglected to study the uncoupling effect. Wave forces were taken to be acting in the direction of surge degree-of-freedom. The geometric properties of the TLP and the hydrodynamic data considered for force evaluation are given in Table 1.

Table 2 shows the coupled and the uncoupled natural time periods of the structure. It is seen that coupling has no effect on natural time periods. It is also observed that TLPs have very long period of vibration associated with motions in the horizontal plane (say 80 to 100 seconds). Since typical

Table 1 Geometric properties of the square TLP and load data

Water properties		Platform properties			
Gravity acceleration (m/sec^2)	9.81	Platform weight (KN),W	280000	Center of gravity above the sea level (m), H_C	6.03
Water weight density (kN/m^3)	10.06	Platform length (m), 2a	66.22	Tether stiffness (KN/m), γ	80000
Inertia coefficient, C_m	2	Platform width (m), 2b	66.22	Tether length (m), L	569
Drag coefficient, C_d	1	Platform radius of gyration in x-directions (m), r_x	32.1	Platform radius of gyration in y-directions (m), r_y	32.1
Current velocity (m/sec), U_c	0	Platform radius of gyration in z-directions (m), r_z	33	Water depth (m), d	600
Wave period (sec), T_w	6, 8, 10, 12.5, and 15	Tether total force (KN), T	160000	Diameter of pontoon (m), D_P	9.03
Wave height (m), H_w	8, 10 and 12	Diameter of columns (m), D_c	18.06	Draft(m),D_r	31
				Damping ratio, ξ	5%

Table 2 Calculated natural structural periods for different analysis cases (in seconds)

Analysis Case	DOF					
	Surge	Sway	Heave	Roll	Pitch	Yaw
Coupled	97.099	97.099	2.218	3.126	3.126	86.047
Uncoupled	97.067	97.067	2.218	3.125	3.125	86.047

wave spectral peaks are between 6 to 15 seconds, resonant response in these degrees of freedom is unlikely to occur.

The natural periods in vertical plane in heave, roll and pitch are observed to be in the range of 2 to 4 seconds which is consistent with typical TLP's. While this range is below the periods of typical storm waves, everyday waves do have some energy in this range (the lowest wave period for most geographical locations is about 3 seconds). Thus, wave–excited vibrations can cause high-cycle fatigue of tethers and eventually instability of the platform. One alternative to this problem is to increase the moored stiffness as to further lower the natural periods in heave, roll and pitch movement. The other alternative is to install damping devices in the tethers to mitigate vertical motion.

Time histories of the coupled and the uncoupled responses are shown in Figs. 8 to 10. Before going into detailed discussion for each response it is clear from the figures that the coupling has no effect on response in the surge and heave directions where, it has negligible effect on pitch direction. This might be attributed to the fact that the hydrodynamic loading was taken as a unidirectional regular wave acting in the surge direction on a symmetrical configuration of the platform.

4.1 Surge response

The time histories of the surge responses for the square TLP are shown in Fig. 8. It is observed that, for a specific wave period, the amplitude of oscillations increases as the wave height increases.

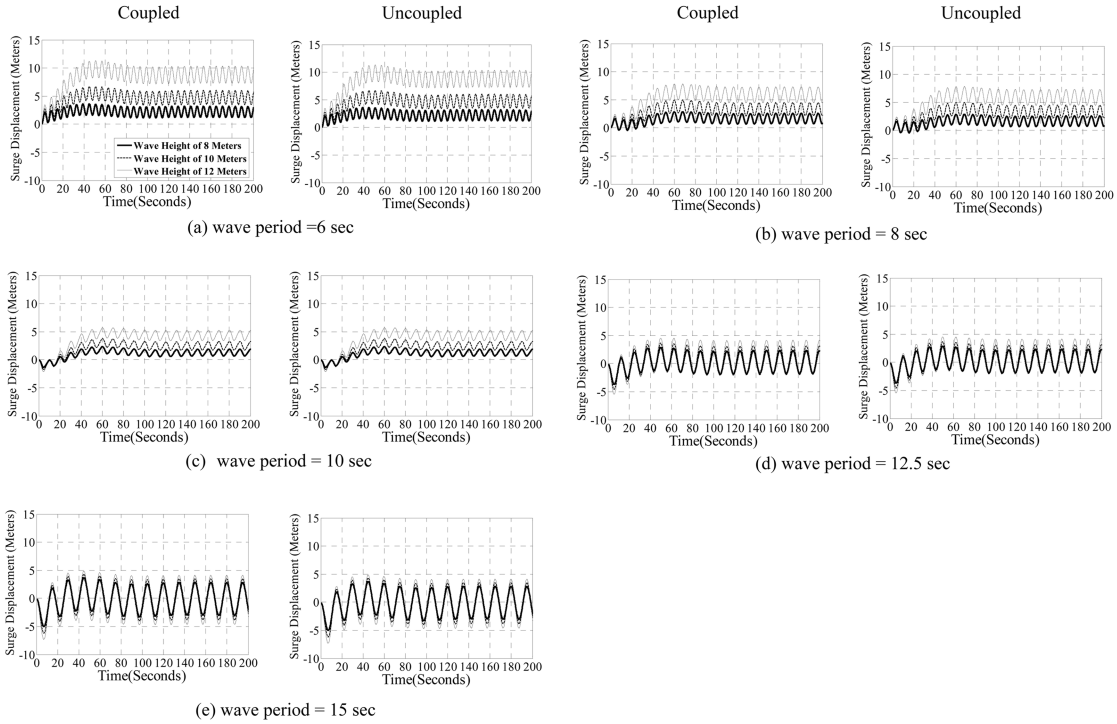

Fig. 8 Surge response of square TLP for (a) wave period = 6 sec, (b) wave period = 8 sec, (c) wave period = 10 sec, (d) wave period = 12.5 sec and (e) wave period = 15 sec

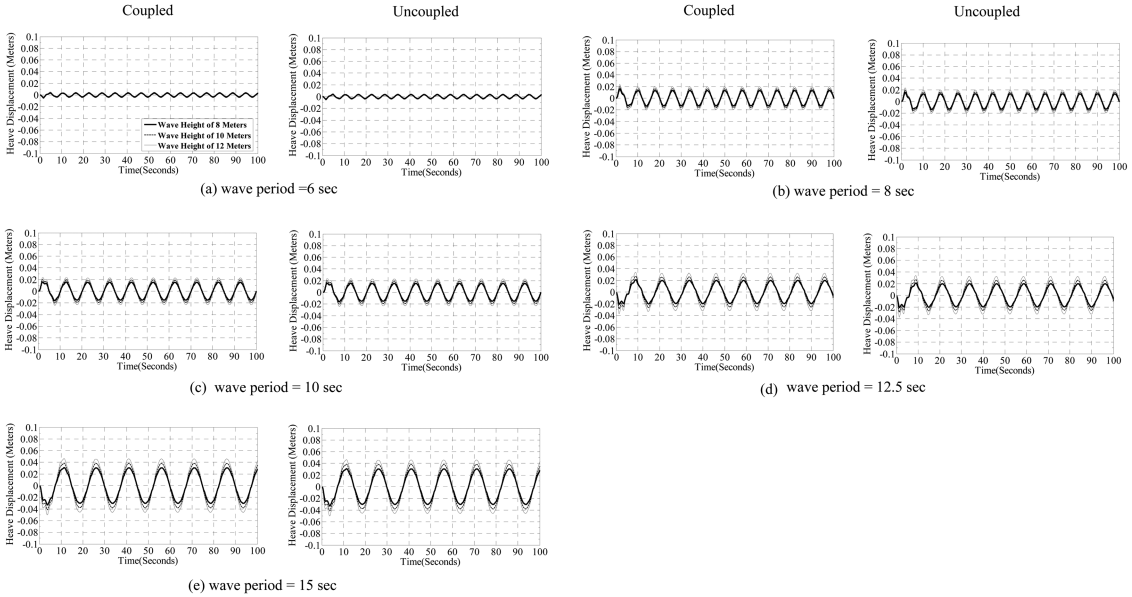

Fig. 9 Heave response of square TLP for (a) wave period = 6 sec, (b) wave period = 8 sec, (c) wave period = 10 sec, (d) wave period = 12.5 sec and (e) wave period = 15 sec

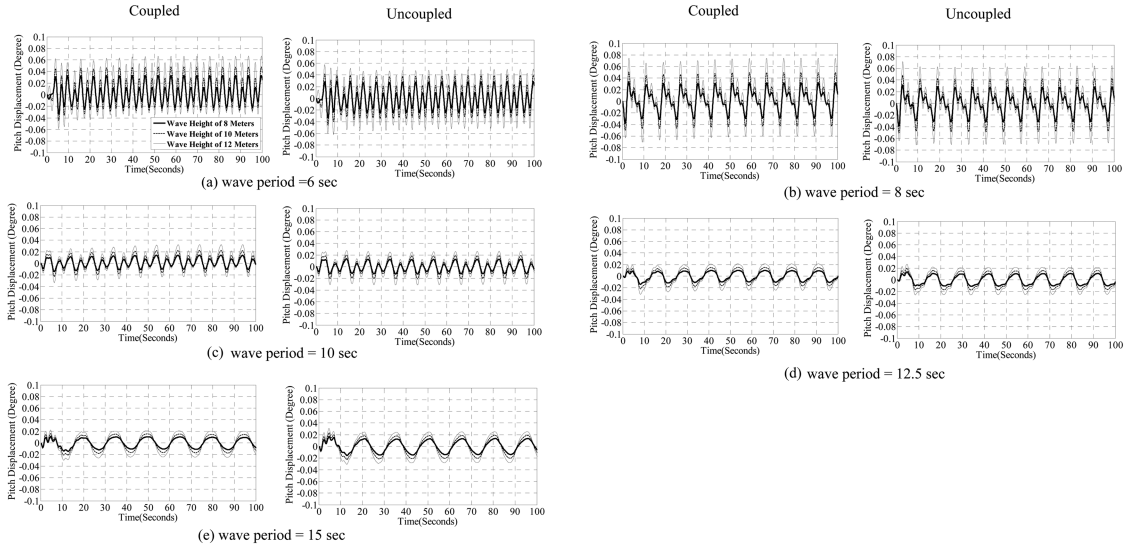

Fig. 10 Pitch response of square TLP for (a) wave period = 6 sec, (b) wave period = 8 sec, (c) wave period = 10 sec, (d) wave period = 12.5 sec and (e) wave period = 15 sec.

Moreover, for short wave periods (up to 10 sec), the system responds in small amplitude oscillations about a displaced position that is inversely proportional to the wave period and directly proportional to wave height. On the other hand, for relatively long wave period (12.5 or 15 sec.), the system tends to respond in high oscillations amplitude about its original position. The amplitude of

oscillations increases with the increase in the wave period, which is expected because as the wave period increases, it becomes closer to the surge period of vibration (about 97 sec.). Moreover, the effect of wave height becomes more pronounced for shorter wave periods. In all cases, the surge response seems to have periodic oscillations that have the same exciting wave period. Finally, the transient state takes about 40-80 seconds where the stationary state begins.

4.2 Heave response

The time histories of the coupled and the uncoupled heave responses are shown in Fig. 9. As expected, the response in the heave direction has very small values compared to that of the surge direction. This is attributed to the relatively high stiffness of the tethers in this direction together with the fact that the excitation is indirect in this case. Moreover, the heave response is directly proportional to the wave period and to a less extent to wave height. Also, the transient state takes about 10 seconds where the stationary state begins and the motion is almost periodic. The heave response appears to have a mean value of nearly zero.

4.3 Pitch response

The time histories of the coupled and the uncoupled pitch responses are shown in Fig. 10. It is clear that as the wave period increases the response becomes closer to being periodic in nature. For short wave periods (up to 10 sec.), a higher mode contribution to the response appears to take place. For long wave periods (12.5 and 15 sec.), the higher mode contribution vanishes after one or two cycles and we have a one period response (wave period) as in the surge and heave cases. Moreover, the transient state takes about 20 seconds before the stationary state begins.

To get an insight into the behavior for the short wave period cases, the response spectra for wave height of 8.0 m and wave period of 6, 8, and 10 sec. was obtained and the results are shown in Fig. 11. Clearly there are three distinct peaks. These are the exciting wave period, a period doubling case in which the spectra have peaks at half the exciting wave periods, and a third peak that is at about one third of the exciting wave period. This particular peak may indicate contribution of the pitch mode of vibration (about 3.1 sec.).

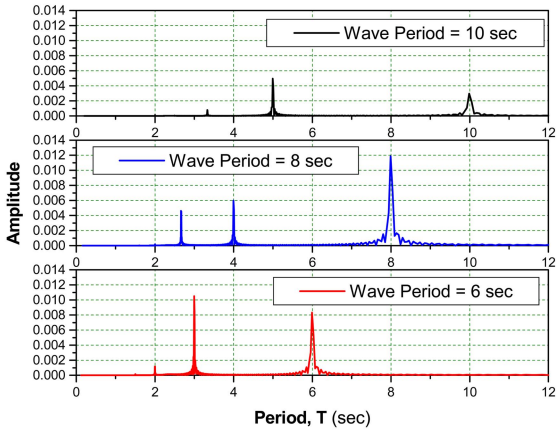

Fig. 11 Response Spectrum for pitch motion for different wave periods (wave height = 8.0 m)

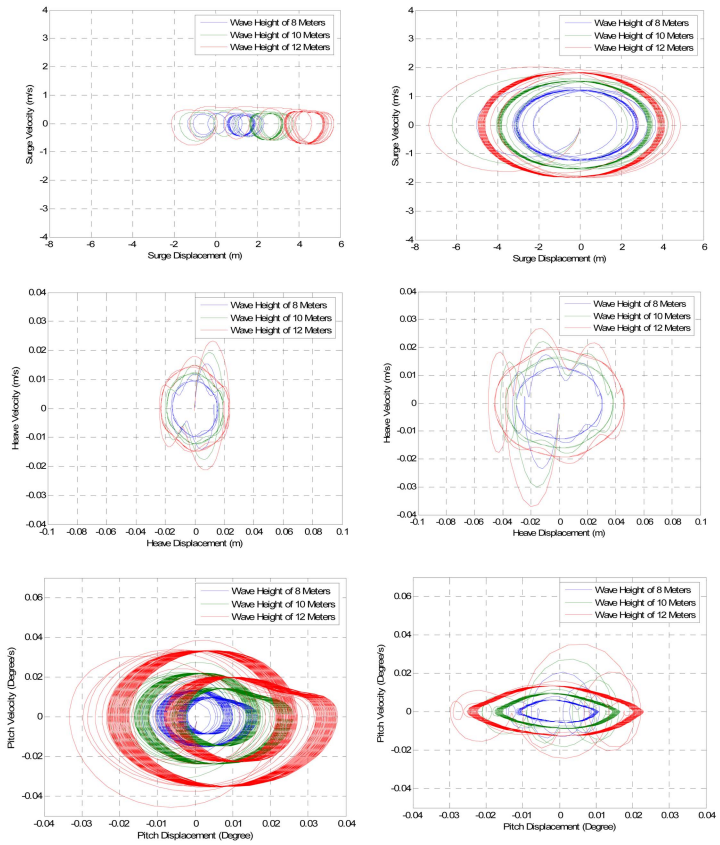

(a) Wave period = 10 sec (b) Wave period = 15 sec

Fig. 12 Phase plane for coupled motion (a) Wave period = 10 sec and (b) wave period = 15 sec

Lastly, to gain a conceptual view of the stability and periodicity of the dynamic behavior of the structure, the phase plane for wave periods of 10 and 15 sec are plotted in Fig. 12. It is observed that the steady state behavior of the structure is periodic and stable.

5. Conclusions

The present study investigates the dynamic response of a square TLP under hydrodynamic forces in the surge direction considering all degrees of freedom of the system. A numerical dynamic model for the TLP was written where Morison's equation with water particle kinematics using Airy's linear wave theory was used. The scope of the work was to accurately model the TLP system considering added mass coefficients and nonlinearity in the system together with the coupling between various degrees of freedom. Results for the time histories for the affected degrees of freedom have been presented. Based on the results shown in this paper, the following conclusions can be drawn:

(1) Given that the hydrodynamic loading is a unidirectional regular wave acting in the surge

direction on a symmetrical configuration of the platform the coupling between various degrees of freedom is insignificant, contrary to the cases of random sea wave loads. Hence, coupling between various degrees of freedom has no effect on the surge or the heave responses, and has an insignificant effect on the pitch response.
(2) TLP's have very long period of vibration (80 to 100 seconds) associated with motions in the horizontal plane, surge, sway and yaw. Since typical wave spectral peaks are between 6 to 15 seconds, resonant response in these degrees of freedom is unlikely to occur.
(3) For short wave periods (less than 10 sec.), the surge response consists of small amplitude oscillations about a displaced position that is inversely proportional to the wave period and directly proportional to wave height. On the other hand, for relatively long wave period (12.5 or 15 sec.), the system tends to respond in high oscillations amplitude about its original position.
(4) The heave response is directly proportional to the wave period and to a less extent to wave height.
(5) For short wave periods (less than 10 sec.), a higher mode contribution to the pitch response accompanied by period doubling appears to take place.
(6) The phase plane shows that the steady state behavior of the structure is periodic and stable.

References

Bhattachatya, S.K., Anitha, J. and Idichandy, V.G. (2004), "Experimental and numerical study of coupled dynamic response of a mini-tension leg platform", *J. Offshore Mech. Arct*., **126**(4), 318-330.
Chandrasekaran, S. and Roy, A. (2005), "Phase space study of offshore structures subjected to non-linear hydrodynamic loading", *Proceedings of the International Conference on Structural Engineering*, SEC 2005, Indian Institute of Science, Bangalore.
Chandrasekaran, S., Jain, A.K., Gupta, A. and Srivastava, A. (2007a), "Response behaviour of triangular tension leg platforms under impact loading", *Ocean Eng*., **34**(1), 45-53.
Chandrasekaran, S., Jain, A.K. and Gupta, A. (2007b), "Influence of wave approach angle on TLP's response", *Ocean Eng*., **34**(8-9), 1322-1327.
Denis. J.P.F. and Heaf, N.J. (1979), "A Comparison between linear and nonlinear response of a proposed tension leg production platform", *Proceedings of the Offshore Technology Conference*, OTC 3555.
Ketabdari, M.J. and Ardakani, H.A. (2005), *Nonlinear response analysis of a sea star offshore tension leg platform in six degrees of freedom*, WIT Transactions on the Built Environment 84.
Kurian, V.J., Gasim, M.A., Narayanan, S.P. and Kalaikumar, V. (2008a), "Parametric study of TLPs subjected to random waves", ICCBT-C-19, 213-222.
Kurian, V.J., Gasim, M.A., Narayanan, S.P. and Kalaikumar, V. (2008b), "Response of square and triangular TLPs subjected to random waves", ICCBT-C-12, 133-140.
Lee, H.H. and Wang, P.W. (2000), "Analytical solution on the surge motion of tension leg twin platform structural systems", *Ocean Eng*., **27**(4), 393-415.
Low, Y.M. (2009), "Frequency domain analysis of a tension leg platform with statistical linearization of the tendon restoring forces", *Mar.Struct*., **22**(3), 480-503.
Morgan, J.R. and Malaeb, D. (1983), "Dynamic analysis of tension leg platforms", *Proceedings of the 2nd international Offshore Mechanics and Arctic Engineering symposium*, USA.
Patel, M.H. (1989), *Dynamics of Offshore Structures*, Butterworth, London.
Tan, S.G. and De Boom, W.C. (1983), "The wave induced motions of a tension leg platform in deep water", *Proceedings of the Offshore Technology Conference*, OTC 4074.
Taudin, P. (1978), "Dynamic response of flexible offshore structures to regular waves", *Proceedings of the Offshore Technology Conference*, OTC 3160.
Yang, C.K. and Kim, M.H. (2010), "Transient effects of tendon disconnection of a TLP by hull–tendon–riser coupled Dynamic analysis", *Ocean Eng*., **37**(8-9), 667-677.